Reduction of the actuator oscillations in the flying vehicle under a follower force

O. Kavianipour[*1], A.M. Khoshnood[2a] and S.H. Sadati[2b]

[1]*Department of Mechanical Engineering, Damavand Branch, Islamic Azad University, Damavand, Iran*
[2]*Department of Aerospace and Mechanical Engineering, K.N.T. University of Technology, Tehran, Iran*

Abstract. Flexible behaviors in new aerospace structures can lead to a degradation of their control and guidance system and undesired performance. The objectives of the current work are to analyze the vibration resulting from the propulsion force on a Single Stage to Orbit (SSTO) launch vehicle (LV). This is modeled as a follower force on a free-free Euler-Bernoulli beam consisting of two concentrated masses at the two free ends. Once the effects on the oscillation of the actuators are studied, a solution to reduce these oscillations will also be developed. To pursue this goal, the stability of the beam model is studied using Ritz method. It is determined that the transverse and rotary inertia of the concentrated masses cause a change in the critical follower force. A new dynamic model and an adaptive control system for an SSTO LV have been developed that allow the aerospace structure to run on its maximum bearable propulsion force with the optimum effects on the oscillation of its actuators. Simulation results show that such a control model provides an effective way to reduce the undesirable oscillations of the actuators.

Keywords: Single Stage to Orbit Launch Vehicle (SSTO LV); beam stability; follower force; vibration reduction; adaptive algorithm

1. Introduction

Many problems are modeled by beams subjected to axial or follower forces. The stability of the beams under the axial or follower force is of vital importance and is in the interests of many researchers as it can be applied to many aerospace structures. The direction of the axial force is assumed to be fixed along the beam while the direction of the follower force is always perpendicular to the cross surface of the beam and changes with the beam deflections. The critical axial force normally causes the static instability (divergence) and the follower force may cause static or dynamic instability (flutter). Divergence happens when the vibration frequency of the system becomes zero and flutter occurs when two natural frequencies of the systems converge together.

The current developments in the aerospace vehicles design have led to produce large flexible structures especially in the new launch vehicles. The larger values of propulsion force-to-weight

---

∗Corresponding author, Ph.D. Student, E-mail: o.kavianipour@gmail.com
[a]Assistant Professor, E-mail: khoshnood@dena.kntu.ac.ir
[b]Assistant Professor, E-mail: sadati@kntu.ac.ir

and length-to-diameter ratios required for long-range flights as well as the cost reduction of handling and launching operation lead to the highly Flexible Launch Vehicles (FLVs). The dynamic response and vibrational characteristics of the FLV are very significant. SSTO LV structure is one of the important models for FLV and is studied as the core model in this study. The SSTO LV structure is modeled by a Euler-Bernoulli beam with two tip masses under the follower and transverse forces that is an acceptable model for such structures with the propulsion and the controller forces (with the actuator forces responsible for the control and guidance of the SSTO LV). The first concentrated mass represents the payload, while the second one stands for the vehicle engine as shown in Fig. 1. One of the objectives pursued in the paper is to determine the maximum follower force structurally bearable in such a way as to prevent instability of the structure. It will be shown that both the transverse and rotary inertia have significant effects on this maximum follower force. On the other hand, flexibility and the elastic behaviors in the SSTO LV can lead to undesired performance and degradation of its control system due to influence of the body vibrations on the Inertial Measurement Units (IMU) measurements. So, in this work, the critical follower force for an SSTO LV model which leads to the instability has been calculated using Ritz method. The effect of the follower force on the vibration in the SSTO LV, and, in particular on its IMU, is then investigated. Also the destructive effect of the vibration of the IMU on oscillation of the SSTO LV actuator in a control loop is presented. Finally an adaptive notch filter is designed and implemented by using Lyapunov theory to develop a new dynamic model and an adaptive control system. The effectiveness of this system is discussed later in this paper.

Beal (1965) investigated a uniform free-free beam under an end follower force. He introduced a direction control mechanism for the follower force to eliminate the tumbling instability of a free-free beam under a follower force. He also showed that, in the absence of a control system, the magnitude of the critical follower force is associated with coalescence of the two lowest bending frequencies. When the control system was included, it was found that the magnitude of the critical follower force only corresponded to a reduction of the lowest frequency of zero. Wu (1975) studied the stability of a free-free beam under a controlled follower force by using finite element discretization with an adjoint formulation. Park and Mote, Jr. (1984) studied the maximum controlled follower force on a free-free beam carrying a concentrated mass. They predicted the location and the magnitude of the additional concentrated mass and the location and the gain of the follower force direction control sensor that permit the follower force to be maximized for stable transverse motion of the beam. Naguleswaran (2004) analyzed the transverse vibration of uniform Euler-Bernoulli beams under linearly varying fully tensile, partly tensile or fully compressive axial force distribution. Thana and Ameen (2007) addressed the dynamic stability problem of columns and frames subjected to the axially-applied periodic loads. The finite element method (FEM) was used in their work to analyze dynamic stability problems of columns. Hassanpour *et al.* (2007) analyzed the exact solution of free vibration of a beam with a concentrated mass within its intervals when the beam was subjected to axial loadings. They determined the exact mode shapes of vibration, which were necessary in the study and analysis of the time-domain response of sensors and determination of stability regions. Pourtakdoust and Assadian (2004) modeled a free-free Bernoulli beam under an axial force. The three dimensional elastic equations of vibration are solved by the FEM. Only the divergence was found and shown in their work. And finally the elastic equations along with the equations of motion were simulated in a controller loop by the authors in their work. It has been shown that the oscillations of the actuators were increased when the axial force was applied. Singh *et al.* (2005) discussed the implementation of axial and follower end forces in a beam-type MEMS resonator for the application of resonant frequency tuning.

Luongo and Di Egidio (2006) studied an internally constrained planar beam, equipped with a lumped visco-elastic device and loaded by a follower force. Paolone *et al.* (2006) analyzed the stability of a cantilever elastic beam with rectangular cross-section under the action of a follower tangential force and a bending conservative couple at the free end. Elfelsoufi and Azrar (2006) presented a mathematical model based on integral equations for numerical investigations of stability analyses of damped beams subjected to sub-tangential follower forces. Many researchers have also published their work on cantilever beam under a follower force with damping (Ryu and Sugiyama 2003, Di Egidio *et al.* 2007, Lee *et al.* 2007). Sugiyama and Langthjem (2007) studied cantilever beam under a follower force with proportional damping. Both internal (material) and external (viscous fluid) damping were considered. Tomski *et al.* (2007) presented the results of theoretical and numerical studies on the slender, geometrically nonlinear system supported at the loaded end by a spring of a linear characteristic and subjected to non-conservative (generalized Beck's) loading. The large-deflection problem of a non-uniform spring-hinged cantilever beam under a tip-concentrated follower force was considered by Shvartsman (2007). Shape optimization was used to optimize the critical load of an Euler-Bernoulli cantilever beam with constant volume subjected to a tangential compressive tip load and/or a tangential compressive load arbitrarily distributed along the beam by Katsikadelis and Tsiatas (2007). De Rosa *et al.* (2008) dealt with the dynamic behavior of a clamped beam subjected to a sub-tangential follower force at the free end. Djondjorov and Vassilev (2008) have studied the dynamic stability of a cantilevered Timoshenko beam lying on an elastic foundation of Winkler type and subjected to a tangential follower force. Attard *et al.* (2008) have investigated the dynamic stability behaviors of damped Beck's columns subjected to sub-tangential follower forces using fifth-order Hermitian beam elements. Marzani *et al.* (2008) have applied the generalized differential quadrature (GDQ) method to solve classical and non-classical non-conservative stability problems. The governing differential equation for a non-uniform column subjected to an arbitrary distribution of compressive sub-tangential follower forces has been obtained. Irani and Kavianipour (2009) investigated effects of a flexible joint on instability of a free-free jointed bipartite beam under the follower and transversal forces. Kavianipour and Sadati (2009) studied effects of damping on the linear stability of a free-free beam subjected to follower and transversal forces.

To reduce the undesired effects of vibration many researchers used optimized control methods in their design of the FLV control systems such as Rynaski (1967), Jenkins and Roy (1968), Maki *et al.* (1972). The optimized control methods included linear and nonlinear in the basis of the minimization of the generalized vibration modes. Bibel and Stalford (1991, 1992) improved gain stabilized mu-controller as well as a control design for a FLV. Englehart and Krause (1992) proposed an analogue notch filter with least square algorithm to reduce the bending vibrational effects on a FLV. Choi and Bang (2000), Choi and Kim (2000) also designed an adaptive control approach to the attitude control of a flexible aerospace system. They used the root mean square method to estimate the bending frequency and one digital notch filter to reduce the flexible behaviors, considering the first and the second bending vibration modes. Ra (2005) proposed a robust adaptive notch filter for a flexible system and Oh *et al.* (2008) examined the attitude control of a FLV using an adaptive notch filter. In another work, Khoshnood *et al.* (2007) proposed a model reference adaptive control for reducing the undesired effects of bending vibration for a FLV. In this study, the approach of Khoshnood *et al.* (2007) is developed in the presence of the follower force which may considerably affect on the parameters of the control system. This work essentially consists of two parts:

Part 1 includes the solution of the elastic equation of the structure in order to find the
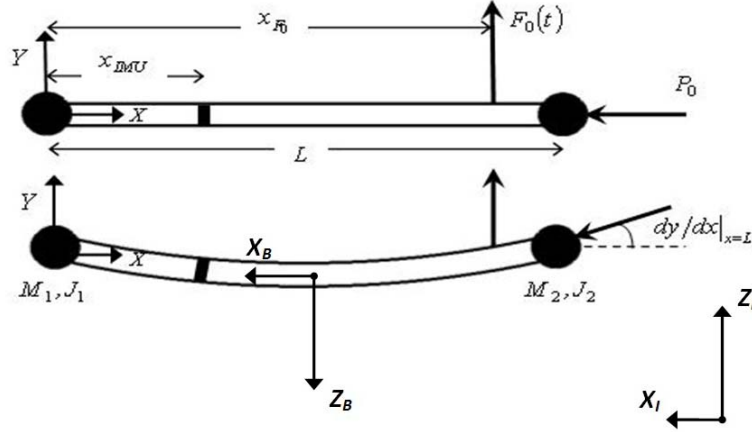
Fig. 1 The simple model of an aerospace structure

propulsion force bearable by the structure. With the particular solution method used (Ritz method), there is a need for the mode shapes for the free-free beam consisting of two concentrated masses at the two free ends.

Part 2 makes use of the linear model for the rigid-elastic body motion and includes the control system for decreasing the vibrations of the actuators.

These two parts are then combined in the end to perform a simulation of the overall controlled system.

2. Mathematical modeling

Fig. 1 shows the assumed model for an aerospace structure. Define the $Z_I X_I$, $Z_B X_B$, and YX as the inertial frame, body frame, and the elastic frame, respectively. The inertial frame is fixed and the body frame and elastic frame are attached to the beam. The mass of the structure is considered to be constant, with no translation of the center of mass of the whole structure. The beam has been assumed to be axially rigid and is an Euler-Bernoulli beam. The gravity force is also ignored. The propulsion force is modeled by a follower force and the transverse force represents the controller force, as shown. In this figure, x_{IMU} and x_{F0} indicate the points on the beam for the locations of the sensors, corresponding to the locations of the Inertial Measurement Units (IMU) and the controller force in the aerospace structure, respectively.

2.1. Energy method

One of the most effective methods to derive the governing equations is the Energy Method. In fact, by considering all the energies in the system and applying the Hamilton's Principle, the governing equations could be derived accurately. The general form of the Hamilton's Principle appears as

$$\delta \int_{t_1}^{t_2} \left(E_k - E_p + W_c \right) dt + \int_{t_1}^{t_2} \delta W_{nc} dt = 0 \tag{1}$$

where δ is the variation, t is the time, E_k is the kinetic energy, E_p is the potential energy, W_c is the work done by conservative forces, and W_{nc} is the work done by non-conservative forces. For the model presented in Fig. 1, Eq. (1) may be presented as

$$
\begin{cases}
E_k = \frac{1}{2}\int_0^L m\left(\frac{\partial y}{\partial t}\right)^2 dx + \frac{1}{2}M_1\left(\frac{\partial y(x=0)}{\partial t}\right)^2 + \frac{1}{2}J_1\left(\frac{\partial^2 y(x=0)}{\partial t \partial x}\right)^2 \\[2mm]
\qquad + \frac{1}{2}M_2\left(\frac{\partial y(x=L)}{\partial t}\right)^2 + \frac{1}{2}J_2\left(\frac{\partial^2 y(x=L)}{\partial t \partial x}\right)^2 \\[2mm]
E_p = \frac{1}{2}\int_0^L EI\left(\frac{\partial^2 y}{\partial x^2}\right)^2 dx \\[2mm]
W_c = \frac{1}{2}\int_0^L P\left(\frac{\partial y}{\partial x}\right)^2 dx \\[2mm]
\delta W_{nc1} = -P_0\left(\frac{\partial y(x=L)}{\partial x}\right)\delta y(x=L) \\[2mm]
\delta W_{nc2} = F_0(t)\delta y\left(x=x_{F_0}\right)
\end{cases}
\tag{2}
$$

In Eq. (2), L is the beam length، m is the beam mass per length, M_1 and M_2 are the first and second concentrated masses, J_1 and J_2 are the rotary inertia of the first and second concentrated masses, EI is the bending stiffness, P is the axial force distribution, P_0 is the follower force, $F_0(t)$ is the transverse force. To calculate the axial force along the beam, the dynamics equilibrium can be used.

$$
\begin{cases}
P = \dfrac{M_1 + mx}{M_1 + mL + M_2}P_0 \quad , \qquad 0 \le x < L \\[3mm]
P = P_0 \qquad\qquad\qquad , \qquad\qquad x = L
\end{cases}
\tag{3}
$$

To simplify the equations, non-dimensional parameters are introduced as the following

$$
\bar{y} = \frac{y}{L} \qquad\qquad \bar{x} = \frac{x}{L} \qquad\qquad \bar{t} = t\left(\frac{EI}{mL^4}\right)^{0.5} \qquad\qquad \bar{P}_0 = \frac{P_0 L^2}{EI}
$$

$$
\bar{F}_0 = \frac{F_0(t)L^2}{EI} \qquad \bar{M}_1 = \frac{M_1}{mL} \qquad \bar{J}_1 = \frac{J_1}{mL^3} \qquad\qquad \bar{M}_2 = \frac{M_2}{mL} \tag{4}
$$

$$
\bar{J}_2 = \frac{J_2}{mL^3}
$$

Considering the fact that the axial force distribution on the beam is not constant, the governing differential equation cannot be solved analytically and an approximation method must be used. Ritz method is the one that has been employed in this study using Hamilton's principle (Hodges and Pierce 2002). In this method the response is approximated with a series as the following

$$
\bar{y}(\bar{x},\bar{t}) = \sum_{i=1}^N \varphi_i(\bar{x})q_i(\bar{t}) \tag{5}
$$

$\varphi_i(\bar{x})$ is admissible function and $q_i(\bar{t})$ is a generalized coordinate.

Replacing Eqs. (3), (4) and (5) in Eqs. (2) and (1), then by simplifying the results and writing the equation in matrix form, Eq. (6) will result as

$$\lfloor M_{ij} \rfloor \lfloor \ddot{q}_j \rfloor + \lfloor K_{ij} \rfloor \lfloor q_j \rfloor = \lfloor Q_j \rfloor \tag{6}$$

where $\ddot{q} = d^2 q / d\bar{t}^2$, $\lfloor M_{ij} \rfloor$ is the mass matrix, $\lfloor K_{ij} \rfloor$ is the stiffness matrix, and $\lfloor Q_j \rfloor$ is the generalized force vector which can be described as

$$
\begin{aligned}
& M_{ij} = \int_0^1 \varphi_i \varphi_j d\bar{x} + \overline{M}_1 \varphi_i(0) \varphi_j(0) + \overline{J}_1 \varphi_i'(0) \varphi_j'(0) + \overline{M}_2 \varphi_i(1) \varphi_j(1) + \overline{J}_2 \varphi_i'(1) \varphi_j'(1) \\
& K_{ij} = \int_0^1 \varphi_i'' \varphi_j'' d\bar{x} - \int_0^1 \overline{P} \varphi_i' \varphi_j' d\bar{x} + \overline{P}_0 \varphi_i'(1) \varphi_j(1) \\
& Q_j = \overline{F}_0 \varphi_j\left(\bar{x}_{F_0}\right)
\end{aligned}
\tag{7}
$$

where $\varphi' = d\varphi / d\bar{x}$ and $\varphi'' = d^2 \varphi / d\bar{x}^2$.

As a common rule, in the approximate solution methods, a partial differential equation may be put into a set of ordinary differential equations.

2.2 Admissible functions

In general the admissible functions should satisfy four conditions:
1) At least must satisfy all geometric boundary conditions.
2) Must be continuous and differentiable to highest spatial derivative.
3) Should be a complete function.
4) Must be linearly independent.
The mode shapes of a free-free beam with two masses at the ends satisfy the above conditions and have been used in this study. As the first two rigid body modes are not involved in the instability, they are not considered as the admissible functions (Beal 1965). It is to be noted that the rigid body modes are controlled by the force in the transverse direction.

$$\varphi_i(\bar{x}) = A_1 Sin(\lambda_i \bar{x}) + A_2 Cos(\lambda_i \bar{x}) + A_3 Sinh(\lambda_i \bar{x}) + A_4 Cosh(\lambda_i \bar{x}) \tag{8}$$

where

$$\lambda_i^4 = \frac{mL^4}{EI} \omega_i^2 \tag{9}$$

and the ω_i is the natural frequency of the model. The A_1, A_2, A_3, and A_4 coefficients are related to the mode shapes and are calculated based on the boundary conditions. The boundary conditions are stated as

$$
\begin{cases}
\varphi''(0) = -\overline{J}_1 \lambda^4 \varphi'(0) \\
\varphi'''(0) = \overline{M}_1 \lambda^4 \varphi(0) \\
\varphi''(1) = \overline{J}_2 \lambda^4 \varphi'(1) \\
\varphi'''(1) = -\overline{M}_2 \lambda^4 \varphi(1)
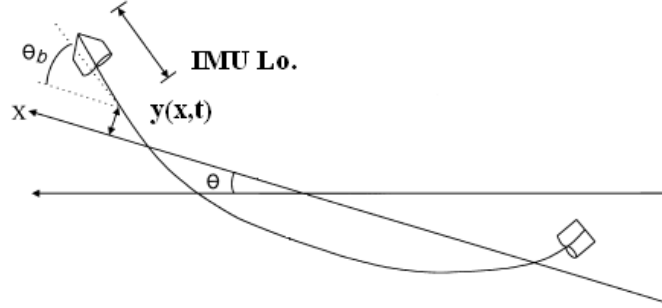\end{cases}
\tag{10}
$$

Fig. 2 Calculation of total pitch angle associated with rigid and elastic motions

3. Rigid body motion and control strategy

The transfer function is first obtained from the rigid body equations for the pitch canal, as described below. The control design for the actuator oscillations is then described.

3.1 Modeling of the pitch channel in the FLV

To model the pitch channel of the FLV in which the elastic behavior follows Eq. (6), one can demonstrate these vibrational effects only in the IMU (Choi and Bang 2000). Hence, the IMU senses the rigid pitch angle associated with the dynamics of the rigid motion as well as the elastic pitch angle associated the Eq. (6). This statement similarly holds for the rate of the pitch angle as shown in Fig. 2.

The slope of the bending vibration deflection can be found by

$$\theta_b = \frac{\partial y(x_{IMU}, t)}{\partial x} = \sum_{i=1}^{N} \varphi_i'(x_{IMU}) q_i(t) \tag{11}$$

where $\varphi_i'(x_{IMU})$ is the slope of the mode shape at the IMU location and θ_b is the magnitude of the bending angle. The total pitch magnitude θ_T is equal to the pitch magnitude of a rigid beam (θ) plus the bending angle expressed as

$$\theta_T = \theta + (-\theta_b) \tag{12}$$

The negative sign in Eq. (12) is related to the particular frames used. The dynamics of the rigid body is presented by deriving the equation of motion for the flight device in the standard format. These equations for the pitch channel in the linear form lead to a third order transfer function. The transfer function between the actuator deflection of the pitch channel (δ_p) and θ is given in the following equation

$$\frac{\theta}{\delta_p} = \frac{-b_1 s + (a_1 b_1 - a_2 b_2)}{s(s^2 - (a_3 + a_4)s + (a_3 a_4 - a_5 a_6))} \tag{13}$$

where a_i and b_j are found from the aerodynamics and system dynamics.

3.2. The main approach to control the actuator oscillations

The main strategy to prevent the destructive effects of the SSTO LV vibrations is to filter the structural dynamics excitation in the closed loop of the rigid control system. In the structures controlled by a closed loop, there are internal excitation sources as well as the external ones that could affect the control system. The internal excitation sources are of vital importance because the continuous interaction of the actuators and the measuring systems involving the vibration of the structure cause the instability or high oscillation on the actuators. This phenomenon can obviously be found in SSTO LVs.

To prevent such destructive effects, the main approach developed in this study is to protect the vibrational bias from feeding back into the control system. Stated differently, it is desirable that the measuring devices do not sense the bending vibration and do not send any excitation feedback to the actuators in all conditions. To this end, the elimination of the vibrational excitation includes two steps: estimation of the bending vibration frequencies, and filtering these frequencies. As the vibration frequencies vary with respect to time, the challenging issue is to estimate them. The approach used in this paper to estimate the bending frequencies is based on the Lyapunov theory and applications in model reference adaptive systems.

Many different filtering methods are available and can be used to filter bending vibrations such as low pass, high pass, and notch filtering. A particular kind of notch filtering has been employed in this research. A simplified infinite impulse response notch filter can be expressed as follows

$$H(z) = \frac{A(z)}{B(z)} = \frac{1 + 2\alpha z^{-1} + z^{-2}}{1 + \alpha(1 + \beta)z^{-1} + \beta z^{-2}} \tag{14}$$

where α is a function of the center frequency of the filter and β is a constant parameter.

Because eight vibration modes of the elastic beam model of SSTO LV are considered in this study, for a first guest, it seems that eight series of filters must be used to reduce the vibrational effects. But as the first and the second modes of vibration are the most active modes and the other ones are in low amplitudes, only two filters can be employed in the control loop with good accuracy. Moreover, with respect to the bandwidth of the closed loop element such as actuator and linear controller, in all conditions, only the main mode of the system dominantly affects the performance of the system. All these considerations have led to the study of designing only one adaptive filter, even though the system consists of more vibrational modes, a claim shown and discussed in later sections of this paper.

3.3 Model reference adaptive system based on Lyapunov theory

In order to estimate the frequency of bending vibration, one can use the rigid model reference adaptive method. This approach is proposed by Khoshnood *et al.* (2007). In their method the stability of algorithm is limited to tune the parameters of the algorithm; hence there are some limitations for increasing the speed of estimation with regard to the value of the parameters. In this paper, the estimation is designed based on the Lyapunov theory to ensure the stability of the algorithm, as shown in Fig. 3.

If the input of the first filter for eliminating the rigid body dynamics is $u(n)$ at the nth step and the output of the pole section is $g(n)$, then
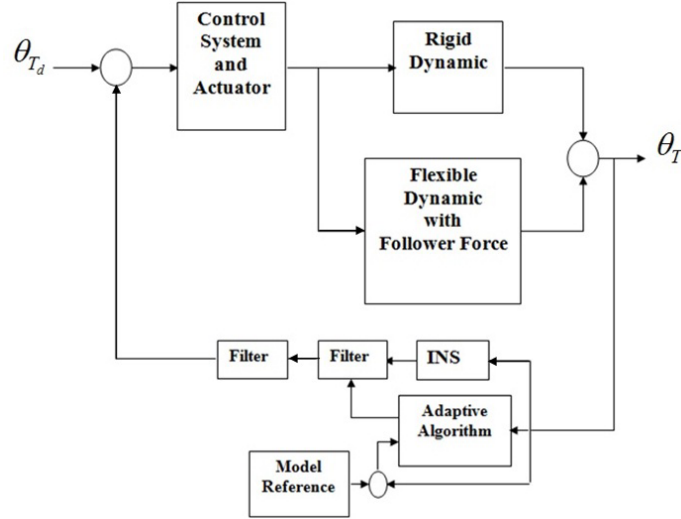
$$g(n) = \frac{1}{B(z)} u(n) \tag{15}$$

Fig. 3 The adaptive algorithm and the control loop

Hence, the output of the filter $w(n)$ can be expressed as

$$w(n) = g(n) + 2\alpha g(n-1) + g(n-2) \tag{16}$$

If w_m indicates the rigid model, the system error can be expressed as

$$e(n) = w_m(n) - w(n) \tag{17}$$

Now, one can select the following function as a Lyapunov function for adaptive algorithm in discrete form as

$$V = \sum_{i=1}^{n} [\frac{1}{2}e^2(n) + \frac{1}{2\gamma}(\alpha(n) - \frac{w_m(n) - g(n) - g(n-2)}{2g(n-1)})^2] \tag{18}$$

where γ is the gain for tuning the speed of estimation.

Considering this Lyapunov candidate, the ΔV can be derived as the following

$$\Delta V = \sum_{i=1}^{n} [\frac{1}{2}e^2(n+1) + \frac{1}{2\gamma}(\alpha(n+1) - \frac{w_m(n+1) - g(n+1) - g(n-1)}{2g(n)})^2$$
$$- \frac{1}{2}e^2(n) - \frac{1}{2\gamma}(\alpha(n) - \frac{w_m(n) - g(n) - g(n-2)}{2g(n-1)})^2] \tag{19}$$

According to the Lyapunov theory, V is a positive function and if

$$\sum_{i=1}^{n} [\frac{1}{2}e^2(n+1) + \frac{1}{2\gamma}(\alpha(n+1) - \frac{w_m(n+1) - g(n+1) - g(n-1)}{2g(n)})^2] = 0 \tag{20}$$

holds, the ΔV can be a semi-negative function. Eq. (20) is then employed to estimate the center frequency of the filter referred to as the frequency of the system.

4. Results and discussion

The results are discussed for several cases as follows.

4.1 Critical follower force

One of the important objective of the present study is to determine the magnitude and type of the least follower force (the divergence or flutter) leading to instability ($\overline{P}_{0cr}$). As seen in Eq. (7), the follower force affects the system stiffness matrix and changes the system frequencies. Therefore, to pursue the stated goal, one must first determine the system frequencies. To obtain the changes in the system frequencies in terms of the follower force, set the right hand side of Eq. (6) to zero ($\overline{F}_0(\bar{t}) = 0$) and assume the homogeneous response as follows.

$$[q_j] = [\hat{q}_j] e^{i\overline{\lambda}\bar{t}} \quad , \quad i = \sqrt{-1} \quad , \quad \overline{\lambda} = \frac{\lambda}{\lambda_1} \tag{21}$$

where $\lfloor \hat{q}_j \rfloor$ is a vector with constant elements and λ_1 is the first non-dimensional system frequency for the case of $\overline{P}_0 = 0$. Therefore, $\overline{\lambda}$ indicates the new non-dimensional system frequency as a result of a change in $\overline{P}_0$. An observation of the two Eqs. (3) and (7) reveals that the concentrated masses have an effect on the system mass matrix and on the system stiffness matrix, and causes a change in the system frequencies. It will be demonstrated that these changes are not predictable. Hence, the effect of these parameters is studied for the following several cases including the:

1) Effect of the $\overline{M}_1$ alone,

2) Effect of the $\overline{M}_2$ alone,

3) Effect of $\overline{M}_1$ and $\overline{M}_2$ together,

4) Effect of $\overline{M}_1$ and $\bar{J}_1$ together,

5) Effect of $\overline{M}_2$ and $\bar{J}_2$ together,

6) Effect of $\overline{M}_1$، $\bar{J}_1$، $\overline{M}_2$ and $\bar{J}_2$ altogether.

To assure the validity of the computer code first, the values of the $\overline{M}_1$, $\bar{J}_1$, $\overline{M}_2$, $\bar{J}_2$ parameters were set to zero for which case it was observed that the resulting instability was of the flutter type, as indeed found by Beal (1965). Moreover, the critical follower force obtained as $\overline{P}_0$ = 109.8 was in fact comparable with $\overline{P}_0$ =109.9 obtained by Beal (1965). It is to be noted that to solve Eq. (6) here in the present work, the first eight mode shapes of the model ($N = 8$) are considered. Fig. 4 depicts the changes in the non-dimensional system frequency versus the non-dimensional follower force for the two specific cases of the parameter values considered. It can be observed that with changes in the system parameters, flutter or divergence occurs and the critical follower force changes as well.

The next few figures show the changes in the critical follower force versus the parameter changes of the model. In each of these figures, the magnitude of the least critical force as well as its type are both indicated. The kink that exists on the curves is due to the transition from flutter to divergence.
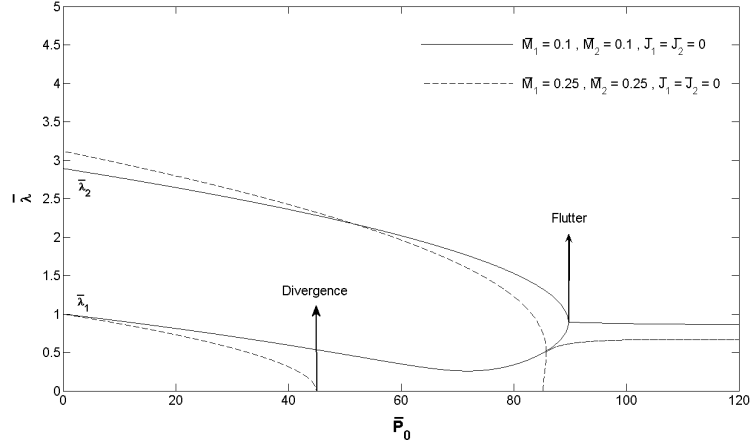
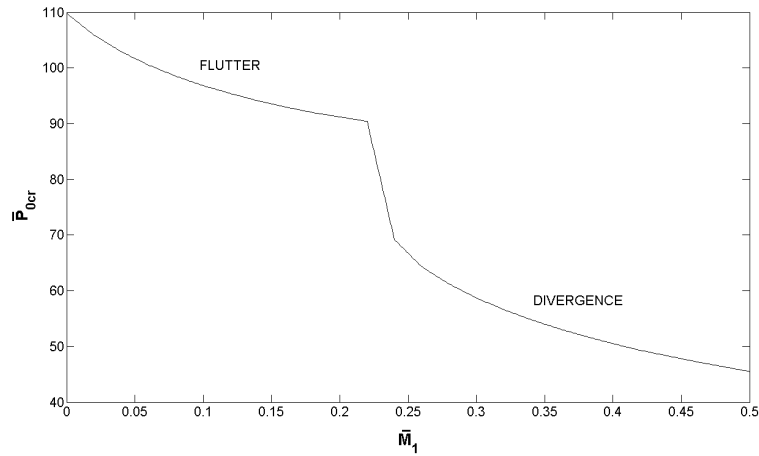Fig. 4 Changes in the non-dimensional system frequency versus the non-dimensional follower

Fig. 5 Changes in the critical follower force for the cases of $\overline{M}_1$ alone

4.1.1 Effect of $\overline{M}_1$ alone

It can be seen in Fig. 5 that flutter occurs for smaller values of $\overline{M}_1$ while divergence occurs for larger values. For the case when flutter occurs, the critical follower force decreases with the increase in $\overline{M}_1$. Also, when divergence occurs too, again the critical follower force decreases with the increase in $\overline{M}_1$.

4.1.2 Effect of $\overline{M}_2$ alone

Fig. 6 indicates that flutter occurs for smaller values of $\overline{M}_2$ while divergence occurs for larger values. For the case when flutter occurs, the critical follower force decreases in the beginning and then starts to increases with the increase in $\overline{M}_2$. Also, when divergence occurs too, again the critical follower force decreases first and then starts to increase as $\overline{M}_2$ increases.
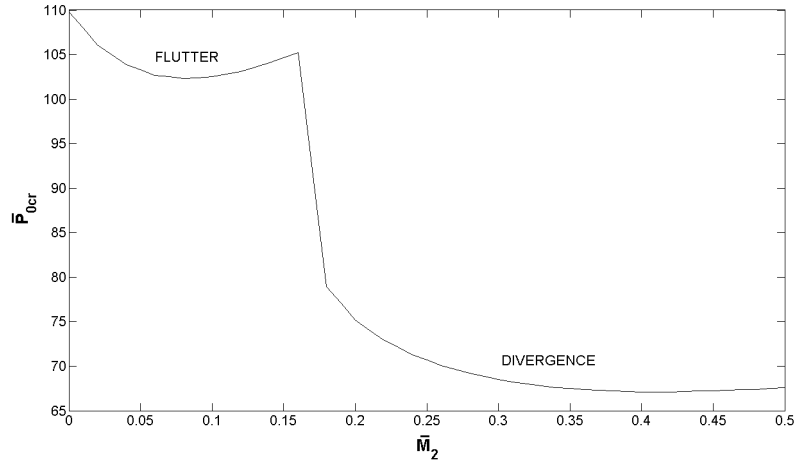
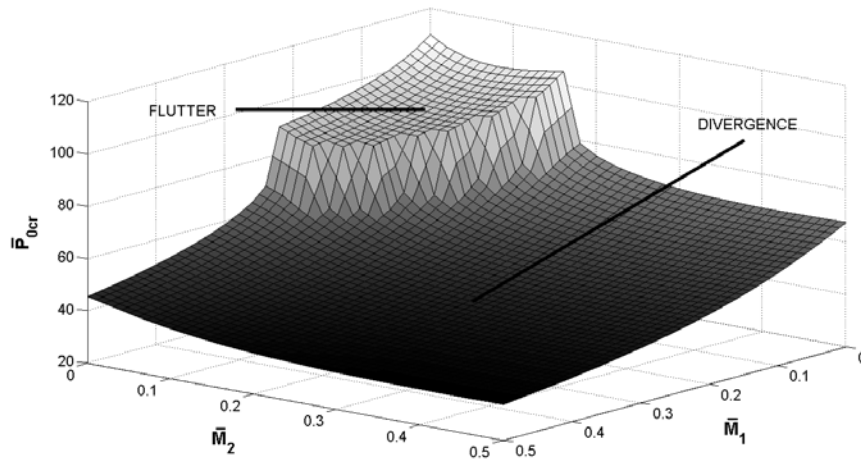Fig. 6 Changes in the critical follower force for the cases of $\overline{M}_2$ alone

Fig. 7 Changes in the critical follower force for the cases of $\overline{M}_1$ and $\overline{M}_2$ together

4.1.3 Effect of $\overline{M}_1$ and $\overline{M}_2$ together

It is observed from Fig. 7 that flutter occurs for smaller values of $\overline{M}_1$ and $\overline{M}_2$ while divergence occurs for larger values. It can be generally inferred in this case that when $\overline{M}_1$ gets larger than a certain value, the critical follower force will decrease with an increase in $\overline{M}_1$ and $\overline{M}_2$.

4.1.4 Effect of $\overline{M}_1$ and $\overline{J}_1$ together

Change in the critical follower force versus $\overline{M}_1$ and $\overline{J}_1$ is shown in Fig. 8. It is quite clear from this figure that when $\overline{M}_1$ is large and $\overline{J}_1$ is small, divergence occurs. For the case when flutter occurs and for a given $\overline{M}_1$, the critical follower force will decrease with the increase in $\overline{J}_1$.
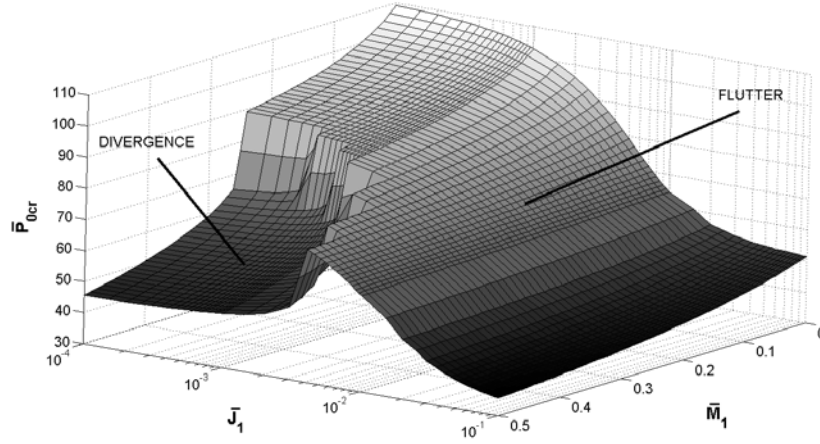
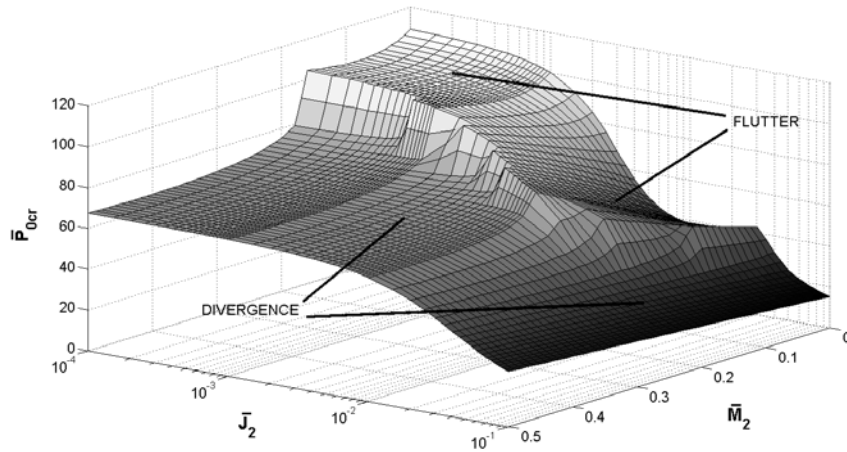Fig. 8 Changes in the critical follower force for the cases of $\overline{M}_1$ and $\overline{J}_1$ together

Fig. 9 Changes in the critical follower force for the cases of $\overline{M}_2$ and $\overline{J}_2$ together

4.1.5 Effect of $\overline{M}_2$ and $\overline{J}_2$ together

Change in the critical follower force versus $\overline{M}_2$ and $\overline{J}_2$ is shown in Fig. 9. It is observed that when $\overline{M}_2$ is large, and also for small values of $\overline{M}_2$ and large values of $\overline{J}_2$, divergence occurs. For the case when divergence occurs and for a given $\overline{M}_2$, the critical follower force will decrease with the increase in $\overline{J}_2$.

4.1.6 Effect of $\overline{M}_1$, $\overline{J}_1$, $\overline{M}_2$ and $\overline{J}_2$ altogether

In this case where the effects of all the parameters are considered, one needs to draw and consider a five-dimensional drawing which is of course impossible. So, a table of variations of the critical follower force versus the related parameters was made up first. Then the maximum and minimum values given in this table were determined. Because of the immense amount of data involved, only the final results have been demonstrated in the table below.

Table 1 Extremum values obtained for the $\overline{M}_1$, $\overline{J}_1$, $\overline{M}_2$ and $\overline{J}_2$ altogether

$\overline{M}_1$	$\overline{J}_1$	$\overline{M}_2$	$\overline{J}_2$	$\overline{P}_{0cr}$
0.35	0.0002	0.35	0.0008	38.7 Divergence (Minimum)
0.15	0.001	0.15	0.0002	83.7 Flutter (Maximum)

Fig. 10 (a) The slope of IMU location versus time, (b) The angle of actuator versus time

4.2 Simulation

One of the objectives of this research is to analyze the displacement of a point in the beam near the tip at which point the Inertial Measuring Units (IMU) is normally located. The analysis of displacements and vibrations of this point over the time is crucial for any control system used in the aerospace structure. The point is shown in Fig. 1 and its distance to the tip of the beam is denoted by x_{IMU}.

To calculate the vibration of the IMU position over the time, one must use dimensional parameters which have been made non-dimensional in the previous sections. One particular case is selected for this analysis which is: $x_{IMU} = 0.1 \times L$, $x_{F0} = L$, $M_1 = 0.15 \times mL$, $J_1 = 0.001 \times mL^3$, $M_2 = 0.15 \times mL$ and $J_1 = 0.0002 \times mL^3$. The first instability for this case ($m = 1.773 \times 10^4$ kg/m, $L = 20$m, $EI = 8.1997 \times 10^{10}$N.m^2) is flutter which occurs when $P_0 = 83.7 \times (EI/L^2)$N.

In Fig. 10, the effects of the follower force on the controller loop are represented. As Figs. 10 (a) and 10 (b) show, the slope at the IMU location and the angle of the actuator increases over the time when the value of the follower force is bigger than that of the critical one, namely ($P_0 = 83.7 \times (EI/L^2)$N). The angle of the actuator becomes saturated because the flutter phenomenon occurred in the structure.

The resulting outcome of applying the adaptive control on the system for $P_0 = 83.7 \times (EI/L^2)$N is shown in Figs. 11 to 13. Fig. 11 presents the frequency estimation using the adaptive algorithm. As shown in this figure, the adaptive algorithm estimates the main active frequency in the SSTO LV vibration properly and the error in recognized frequency is low and acceptable. The variations of the angle of the actuator in two cases (with and without adaptive controller) are shown in Fig. 12. The oscillation of the actuator is obviously reduced when the adaptive controller is applied. Fig. 13 shows the variations of the angle of the IMU in the system while the adaptive control system is
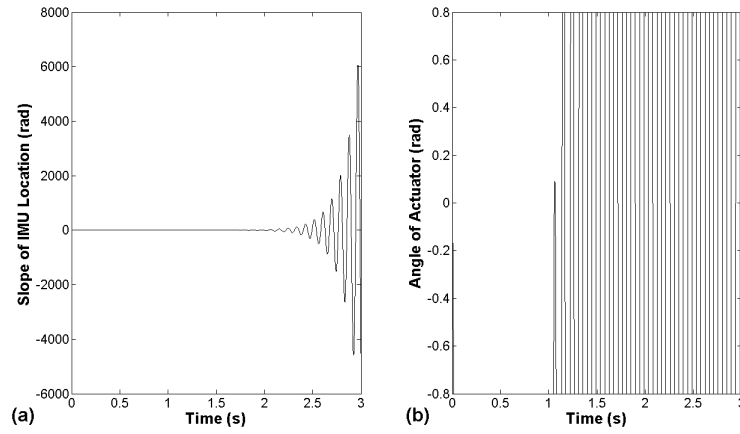
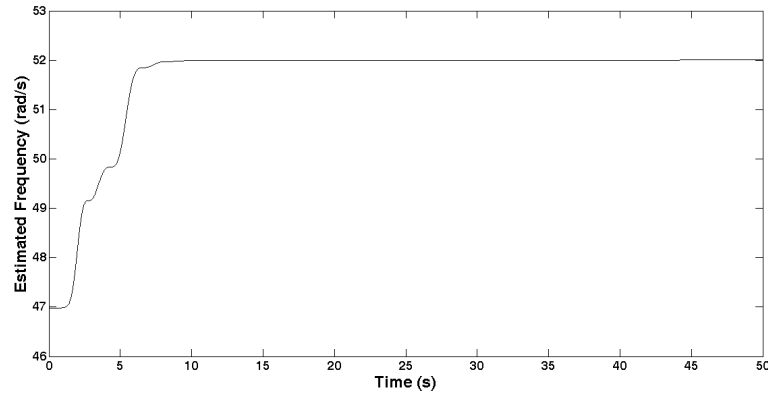Fig. 10 (a) The slope of IMU location versus time, (b) The angle of actuator versus time

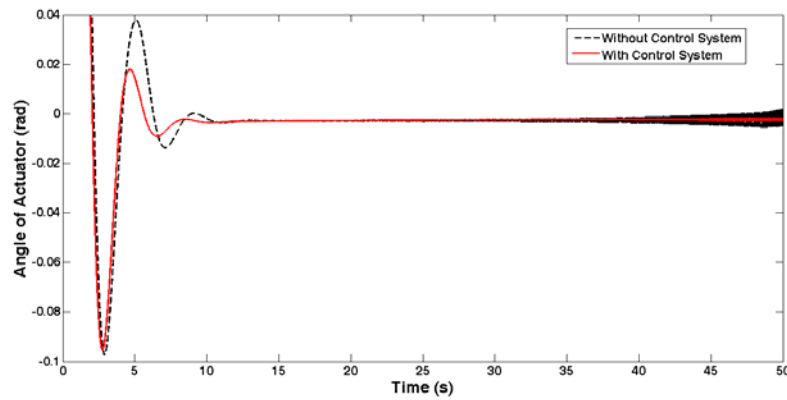Fig. 11 The frequency estimation using the adaptive algorithm

Fig. 12 The variations of the angle of the actuator in two cases (with and without adaptive controller)

applied and also is compared with the same variations without the controller. This figure shows that the controller was able to limit the vibration of the IMU while it was divergent when no controller was applied.
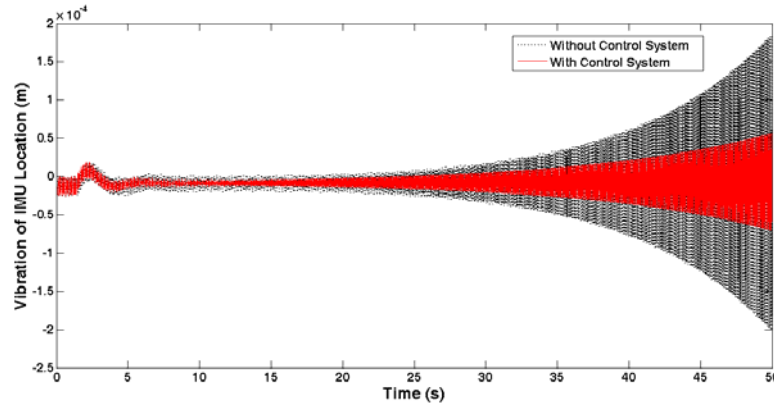
Fig. 13 Comparison of the vibration of IMU location in the system with and without adaptive controller

5. Conclusions

In this paper the stability and vibrations of a free-free Euler-Bernoulli beam with two tip masses at the ends, i.e., the SSTO structure, under the follower and transverse forces have been analyzed. The follower force is the model for the propulsion force and the transverse force is the controller force. The first concentrated mass represents the payload, while the second one stands for the vehicle engine. Both the transverse and rotary inertia of the concentrated masses have notable effects on the stability of the beam, causing a change in the magnitude of the critical follower force ($\overline{P}_{0cr}$) and the type of the ensuing instability, as shown in section 4.1. In this work, the effect of these parameters has been studied using Ritz method for the following six cases including:

1) Effect of the $\overline{M}_1$ alone, 2) Effect of the $\overline{M}_2$ alone, 3) Effect of $\overline{M}_1$ and $\overline{M}_2$ together, 4) Effect of $\overline{M}_1$ and $\overline{J}_1$ together, 5) Effect of $\overline{M}_2$ and $\overline{J}_2$ together, 6) Effect of $\overline{M}_1, \overline{J}_1, \overline{M}_2$, and $\overline{J}_2$ altogether.

To complete the design process, the values for the $\overline{M}_1$, $\overline{J}_1$, $\overline{M}_2$ and $\overline{J}_2$ must be determined, as used in Eq. (7) while $\overline{P}_{0cr}$ becomes maximum. This is done by solving the governing equation first, followed by making up a table of variations of the critical follower force versus the related parameters. This table was not presented in the paper and only the final results have been demonstrated. The results of this paper offer an approximation method to design the two concentrated masses at the ends of a beam under the follower force.

The destructive effects of the bending vibration of an SSTO LV (when the follower force is considered) on its control system and in particular on the undesirable oscillations of its actuator are also studied. In this work, the equation of motion of elastic bending vibration of the SSTO LV having a follower force is derived and added to a control system. It has been shown that the effects of the bending vibration on oscillations of the actuators are of vital importance and when the follower force is increased, the oscillation of the actuators also increases considerably. To reduce these negative effects, the bending vibration of the SSTO LV was modeled using the eight mode shapes and regarding to only one dominant frequency of the system, an adaptive notch filter could

almost omit the bending vibration of the IMU location from the control system. The results of the current work show that this strategy which has been successfully employed in the previous models without any follower force influences can reduce the negative effects of the structural vibrations, especially in the presence of any follower force effects. Moreover, it has been demonstrated that by using this system, one can have the maximum follower force (less than critical follower force) in an SSTO LV and control the high amplitude vibration of the IMU location.

Acknowledgements

References

Attard, M.M., Lee, J.S. and Kim, M.Y. (2008), "Dynamic stability of shear-flexible beck's columns based on Engesser's and Haringx's buckling theories", *Computers and Structures*, **86**, 2042-2055.

Beal, T.R. (1965), "Dynamic stability of a flexible missile under constant and pulsating thrusts", *AIAA Journal*, **3**, 486-494.

Bibel, J. and Stalford, H. (1991), "Mu-synthesis autopilot design for a flexible launch vehicle", *AIAA-19371, 29th Aerospace Sciences Meeting*, Nevada, January.

Bibel, J. and Stalford, H. (1992), "An improved gain stabilized Mu-controller for a flexible launch vehicle", *AIAA-92-0206, 30th Aerospace Sciences Meeting & Exhibit*, NV, January.

Choi, H.D. and Bang, H. (2000), "An adaptive control approach to the attitude control of a flexible rocket", *Control Engineering Practice*, **8**, 1003-1010.

Choi, H.D. and Kim, J. (2000), "Adaptive notch filter design for bending vibration of a sounding rocket", *Aerospace Engineering journal of IMechE*, **215**, 13-23.

De Rosa, M.A., Auciello, N.M. and Lippiello, M. (2008), "Dynamic stability analysis and DQM for beams with variable cross-section", *Mechanics Research Communications*, **35**, 187-192.

Di Egidio, A., Luongo, A. and Paolone, A. (2007), "Linear and non-linear interactions between static and dynamic bifurcations of damped planar beams", *International Journal of Non-Linear Mechanics*, **42**, 88-98.

Djondjorov, P.A. and Vassilev, V.M. (2008), "On the dynamic stability of a cantilever under tangential follower force according to Timoshenko beam theory", *Journal of Sound and Vibration*, **311**, 1431-1437.

Elfelsoufi, Z. and Azrar, L. (2006), "Integral equation formulation and analysis of the dynamic stability of damped beams subjected to subtangential follower forces", *Journal of Sound and Vibration*, **296**, 690-713.

Englehart, M.J. and Krause, J.M. (1992), "An adaptive control concept for flexible launch vehicles", *AIAA-92-4622-CP*, 1505-1512.

Hassanpour, P.A., Cleghorn, W.L., Mills, J.K. and Esmailzadeh, E. (2007), "Exact solution of the oscillatory behavior under axial force of a beam with a concentrated mass within its interval", *Journal of Vibration and Control*, **13**, 1723-1739.

Hodges, D.H. and Pierce, G. A. (2002), *Introduction to Structural Dynamics and Aeroelasticity*, The Press Syndicate of The University of Cambridge, Cambridge.

Irani, S. and Kavianipour, O. (2009), "Effects of a flexible joint on instability of a free-free jointed bipartite beam under the follower and transversal forces", *Journal of Zhejiang University Science A*, **10**(9), 1252-1262.

Jenkins, K.W. and Roy, R.J. (1968), "Pitch control of a flexible launch vehicle", *IEEE Transaction on*

Automatic Control, SHORT PAPERS, 181-186.

Kavianipour, O. and Sadati, S.H. (2009), "Effects of damping on the linear stability of a free-free beam subjected to follower and transversal forces", *Structural Engineering and Mechanics*, **33**(6), 709-724.

Katsikadelis, J.T. and Tsiatas, G.C. (2007), "Optimum design of structures subjected to follower forces", *International Journal of Mechanical Sciences*, **49**, 1204-1212.

Khoshnood, A.M., Roshanian, J. and Khaki-Sedigh, A. (2007), "Model reference adaptive control for a flexible launch vehicle", *Journal of Systems and Control Engineering*, **222**, 45-52.

Lee, J.S., Kim, N.I. and Kim, M.Y. (2007), "Sub-tangentially loaded and damped Beck's columns on two-parameter elastic foundation", *Journal of Sound and Vibration*, **306**, 766-789.

Luongo, A. and Di Egidio, A. (2006), "Divergence, Hopf and double-zero bifurcations of a nonlinear planar beam", *Computers and Structures*, **84**, 1596-1605.

Maki, M.C. and Van De Vegte, J. (1972), "Optimal and constrained-optimal control of a flexible launch vehicle", *AIAA Journal*, **10**, 796-799.

Marzani, A., Tornabene, F. and Viola, E. (2008), "Nonconservative stability problems via generalized differential quadrature method", *Journal of Sound and Vibration*, **315**, 176-196.

Naguleswaran, S. (2004), "Transverse vibration of a uniform Euler-Bernoulli beam under linearly varying axial force", *Journal of Sound and Vibration*, **275**, 47-57.

Oh, C.S., Bang, H. and Park, C.S. (2008), "Attitude control of a flexible launch vehicle using an adaptive notch filter: ground experiment", *Control Engineering Practice*, **16**, 30-42.

Paolonea, A., Vastab, M. and Luongoc, A. (2006), "Flexural-torsional bifurcations of a cantilever beam under potential and circulatory forces I. Non-linear model and stability analysis", *International Journal of Non-Linear Mechanics*, **41**, 586-594.

Pourtakdoust, S.H. and Assadian, N. (2004), "Investigation of thrust effect on the vibrational characteristics of flexible guided missiles", *Journal of Sound and Vibration*, **272**, 287-299.

Ra, W.S. (2005), "Practical adaptive notch filter of missile bending mode rejection", *IEEE Electronic letters*, **41**(5).

Ryanski, E.G. (1967), "Optimal control of flexible launch vehicle", *AIAA paper*, No. 67-592, Guidance, Control and Flight Dynamics Conference HUNTSVILLE, Alabama, August.

Ryu, S.U. and Sugiyama, Y. (2003), "Computational dynamics approach to the effect of damping on stability of a cantilevered column subjected to a follower force", *Computers and Structures*, **81**, 265-271.

Singh, A., Mukherjee, R., Turner, K. and Shaw, S. (2005), "MEMS implementation of axial and follower end forces", *Journal of Sound and Vibration*, **286**, 637-644.

Sugiyama, Y. and Langthjem, M.A. (2007), "Physical mechanism of the destabilizing effect of damping in continuous non-conservative dissipative systems", *International Journal of Non-Linear Mechanics*, **42**, 132-145.

Thana, H.K. and Ameen, M. (2007), "Finite element analysis of dynamic stability of skeletal structures under periodic loading", *Journal of Zhejiang University Science A*, **8**, 245-256.

Tomski, L., Szmidla, J. and Uzny, S. (2007), "The local and global instability and vibration of systems subjected to non-conservative loading", *Thin-Walled Structures*, **45**, 945-949.